Open Journal of Applied Sciences, 2025, 15(4), 773-783
https://www.scirp.org/journal/ojapps
ISSN Online: 2165-3925
ISSN Print: 2165-3917

Dynamic Similarity Optimization Design of an Aero-Engine

Zuxin Chen, Fei Wang*, Shan Zeng, Yancong Lin

School of Power and Energy, Nanchang Hangkong University, Nanchang, China
Email: *70747@nchu.edu.cn

How to cite this paper: Chen, Z.X., Wang, F., Zeng, S. and Lin, Y.C. (2025) Dynamic Similarity Optimization Design of an Aero-Engine. *Open Journal of Applied Sciences*, **15**, 773-783.
https://doi.org/10.4236/ojapps.2025.154051

Received: March 7, 2025
Accepted: March 24, 2025
Published: March 27, 2025

Abstract

Aiming at the dynamic similarity design of an aero-engine rotor system, this study proposes a parameterized dynamic similarity design method based on a genetic algorithm, specifically addressing the dynamic equivalence issues between compressor and turbine disk structures. Taking the first three critical speeds of the prototype engine as objective functions, the thickness and diameter parameters of compressor stages and turbine disks were parameterized. Optimization design variables and constraints were established to formulate a dynamic similarity optimization model. By constructing a MATLAB-ANSYS cross-platform collaborative optimization framework, a genetic algorithm-driven single-objective parameter optimization mechanism was developed to iteratively optimize key structural parameters of the model rotor, ultimately obtaining a simplified rotor model dynamically equivalent to the prototype. Results demonstrate that the derived dynamic similarity model effectively predicts the dynamic characteristics of the prototype engine, with relative errors of 0.95%, 0.98%, and 0.28% for the first three critical speeds respectively. Moreover, the first three critical vibration modes show complete consistency, providing a reliable approach for subsequent vibration control in aero-engine rotor systems.

Keywords

Aero-Engine, Dynamic Similarity, Genetic Algorithm, Rotor System

1. Introduction

The operational conditions of aero-engines are characterized by multi-physics coupling (high-speed rotation, high-temperature environments, and aerodynamic loads), wide-band dense modal distribution, aeroelastic interaction effects, and multi-path energy transfer [1]. Consequently, vibration issues have always been a critical constraint in engine development. According to statistics, vibration-induced engine failures account for 50% - 60% of total engine malfunctions, making effective vibration suppression a core objective for improving engine reliability and extending service life [2]-[6]. Dynamic similarity design holds unique advantages in aero-engine vibration control, particularly in addressing dynamic mismatch caused by multi-stage rotor systems and structural modifications.

However, existing research primarily focuses on dynamic similarity design for simplified rotor systems [7] [8], achieving critical speed matching by adjusting mass, stiffness, and damping parameters. While such methods have advanced fundamental research, they struggle to be directly applied to practical aero-engine rotor systems involving multi-stage compressors, turbine disks, and complex support structure coupling.

This paper takes a specific aero-engine as the research object and focuses on the design of its dynamic similarity model, proposing a genetic algorithm-based optimization method for rotor system modeling. This approach breaks through the limitations of simplified rotor systems by establishing a parameterized model for multi-stage disk-support coupling, significantly improving critical speed prediction accuracy. First, the objective function is defined based on the first three critical speeds of the engine. Next, parameters such as compressor stages, turbine components, and support stiffness are parameterized, with optimization design parameters and constraints established. Finally, MATLAB-ANSYS co-simulation is utilized to optimize the dynamic similarity model, ensuring alignment with the prototype engine's critical speeds.

2. Prototype Rotor System

The research object of this paper is a certain type of aero-engine rotor system, whose structure is shown in **Figure 1**. It consists of a four-stage axial compressor, a single-stage centrifugal compressor, a two-stage turbine, a hollow tie-rod shaft, and corresponding support systems. The rotor section adopts a drum-type configuration, where disks, blades, and the rotating shaft form the main power transmission components. The Campbell diagram of this aero-engine is presented in **Figure 2**, with the first three critical speeds being 7913 rpm, 15,337 rpm, and 55,721 rpm respectively.

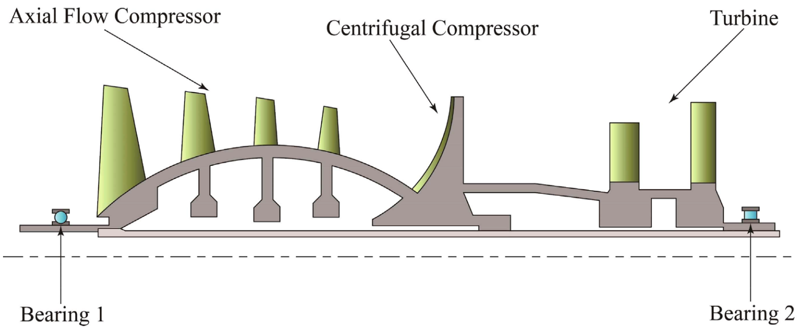

Figure 1. Rotor diagram of a certain type of aero-engine.

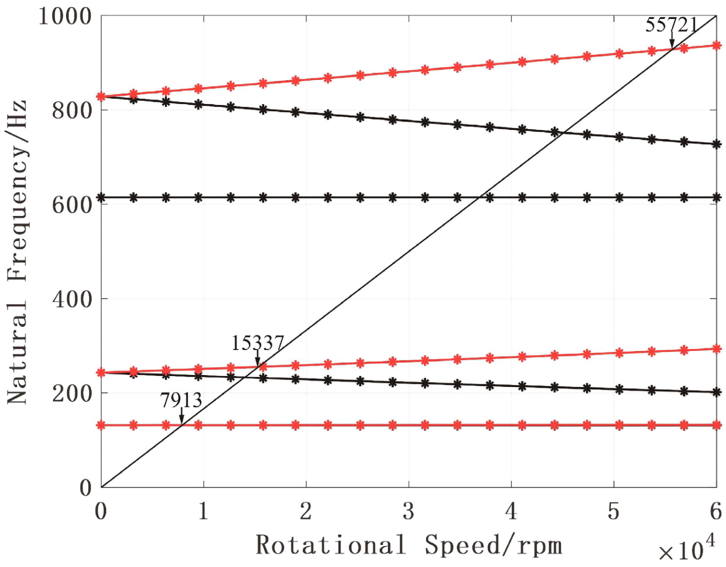

Figure 2. Campbell diagram of a certain type of aero-engine.

3. Establishment of the Dynamic Similarity Model

3.1. Critical Speed Solution

The equation of motion of the rotor system can be written as:

$$\boldsymbol{M}_R\ddot{\boldsymbol{u}}+\left(\boldsymbol{C}_B+\Omega\boldsymbol{G}_R\right)\dot{\boldsymbol{u}}+\left[\boldsymbol{K}_R+\boldsymbol{K}_B\right]\boldsymbol{u}=\boldsymbol{Q} \tag{1}$$

here, the subscripts R and B denote contributions from the rotor and support, respectively. $\boldsymbol{M}$, $\boldsymbol{K}$, $\boldsymbol{C}$, and $\boldsymbol{G}$ represent the mass matrix, stiffness matrix, damping matrix, and gyroscopic matrix, respectively, while $\boldsymbol{Q}$ denotes the load vector.

The critical speeds of the rotor system can be determined using Equation (1) through methods such as the Campbell diagram method and the characteristic equation method. The mathematical principles of the characteristic equation method are described as follows:

For rotor systems, the frequencies of excitation forces acting upon the system are invariably expressible in the following form:

$$\omega_f=n\Omega \tag{2}$$

where Ω denotes the rotational speed of the rotor. According to Equation (2), the excitation force acting on the rotor system can be expressed as:

$$\boldsymbol{Q}(t)=\boldsymbol{Q}_0\mathrm{e}^{j\omega_f t} \tag{3}$$

The rotor system response induced by this excitation force can be written as:

$$\boldsymbol{u}(t)=\boldsymbol{u}_0\mathrm{e}^{j\omega_f t} \tag{4}$$

Substituting Equations (2)-(4) into Equation (1) gives:

$$\boldsymbol{D}\boldsymbol{u}_0=\boldsymbol{Q}_0 \tag{5}$$

where:

$$\boldsymbol{D} = -\Omega^2\left[n^2\boldsymbol{M} - jn\boldsymbol{G}\right] + j\Omega n\boldsymbol{C} + \boldsymbol{K} \tag{6}$$

The characteristic equation method solves the eigenvalue problem for $n = 1$. To calculate critical speeds, set $n = 1$ and construct matrix $\boldsymbol{A}$:

$$\boldsymbol{A} = \begin{bmatrix} \boldsymbol{0} & \boldsymbol{I} \\ -\boldsymbol{M}_v^{-1}\boldsymbol{K}_v & -\boldsymbol{M}_v^{-1}\boldsymbol{C}_v \end{bmatrix} \tag{7}$$

where:

$$\begin{cases} \boldsymbol{M}_v = -\boldsymbol{M} + j\boldsymbol{C} & \boldsymbol{M} = \boldsymbol{M}_R \\ \boldsymbol{K}_v = \boldsymbol{K} = \boldsymbol{K}_R + \boldsymbol{K}_B & \boldsymbol{C} = \boldsymbol{C}_B \\ \boldsymbol{C}_v = j\boldsymbol{C} & \boldsymbol{C} = \boldsymbol{C} \end{cases} \tag{8}$$

The critical speeds of the rotor system can be obtained by solving the eigenvalues of the system matrix. In Equation (8), $j = \sqrt{-1}$ denotes the imaginary unit. The characteristic equation method requires only a single eigenvalue solution to determine all critical speeds of the system, demonstrating superior computational efficiency and enhanced suitability for rotor critical speed optimization.

3.2. Establishment of the Objective Function

Critical speed is the core index reflecting the dynamic characteristics of the rotor system, this paper takes the first three orders of critical speed of this engine as the optimization objective function, as shown in Equation (9):

$$obj = \min \sum_{i=1}^{3} \frac{\left| \frac{\omega_i}{\lambda} - \Omega_i \right|}{\Omega_i} \tag{9}$$

where $\lambda = 1.0$ is the specified similarity ratio; $\omega_i, i = 1, 2, 3$ is the first three orders of critical speed of the model rotor system; $\Omega_i, i = 1, 2, 3$ is the first three orders of critical speed of the aero-engine rotor system.

3.3. Establishment of the Dynamic Similarity Model

Optimization algorithms can be broadly classified into exact algorithms and heuristic algorithms. Gradient-based optimization algorithms utilize gradient information of the objective function to iteratively approach optimal solutions through local derivative analysis. These methods are characterized by high computational efficiency and rapid convergence rates, making them particularly suitable for low-dimensional, continuous, smooth convex optimization problems. However, their effectiveness depends on the differentiability of the objective function and they are prone to local optima trapping.

In contrast, heuristic algorithms employ stochastic search mechanisms inspired by natural phenomena or swarm behaviors to achieve global exploration. These gradient-free methods demonstrate strong capability in handling high-dimensional, non-convex, multimodal, or discrete-variable optimization problems, exhibiting enhanced robustness and potential for global convergence.

As a heuristic algorithm, Genetic Algorithm (GA) translates biological evolutionary principles—specifically the "survival of the fittest"—into mathematical optimization processes via fitness function mapping mechanisms. Its unique encoding-decoding strategies and swarm intelligence characteristics endow it with exceptional global exploration capabilities in solving complex nonlinear optimization problems.

In the context of rotor system model design based on genetic optimization algorithms, similarity-related challenges are transformed into computable optimization problems. This approach effectively resolves model construction difficulties under incomplete similarity conditions, offering a methodological framework for developing testbench systems for highly complex dynamic systems.

The objectives of rotor system dynamic optimization design include:

1) Adjusting critical speeds to ensure the optimized rotor's operational speed maintains sufficient safety margins, effectively avoiding its critical speed ranges;

2) Optimizing the structural parameters of the model rotor to minimize vibration amplitude under operational conditions.

Design variables, as the core adjustable parameters influencing the optimization scheme, directly determine the validity of the optimization results. The total number of variables corresponds to the dimensionality of the optimization problem. To ensure engineering applicability, all design variables must be assigned reasonable numerical constraint ranges.

A rotor system typically consists of three fundamental components: rigid discs, rotating shafts, and support bearings. Each component can be treated as an independent similarity unit, with similarity characteristics categorized into geometric configuration similarity and kinetic performance similarity. Among these, geometric configuration similarity (structural morphology) plays a dominant role in the similarity analysis of rotor systems, as illustrated in **Figure 3**.

For the studied aero-engine rotor system, its characteristic parameters include:

1) Diameter and thickness of 3 axial compressor discs,

2) Outer diameter and thickness of 1 centrifugal compressor disc,

3) Outer diameter and thickness of 2 turbine discs.

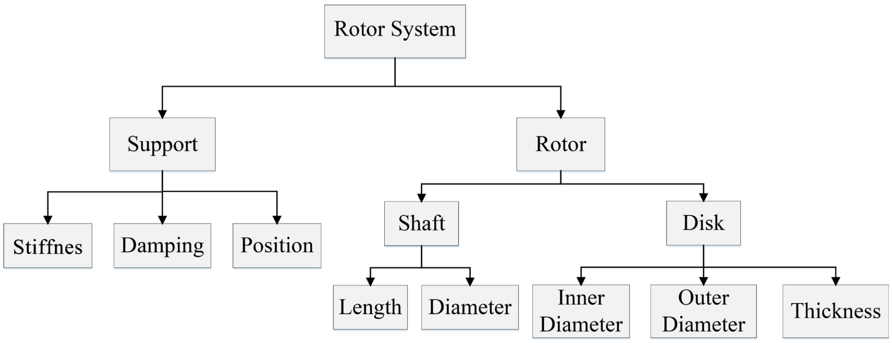

Figure 3. Characteristic parameters of the rotor system.

To achieve the optimization design objectives, the thickness similarity constants and diameter similarity constants of each disc in the rotor system are selected as optimization design variables. Based on the rotor system's overall performance and structural characteristics, the chosen optimization variables are illustrated in **Figure 4**, with their respective value ranges summarized in **Table 1**.

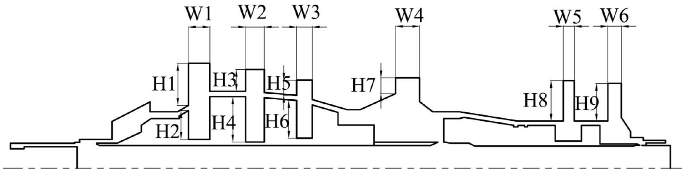

Figure 4. Schematic of design variables.

Table 1. Range of values for design variables.

design variables	H1	H2	H3	H4	H5	H6	H7	H8
Range of values, mm	19.5 - 65	1 - 40	1 - 30	1 - 64	1 - 45	1 - 56	12 - 30	5 - 70
design variables	H9	W1	W2	W3	W4	W5	W6	
Range of values, mm	5 - 70	5 - 75	5 - 50	34 - 27	5 - 79	5 - 36	5 - 29	

The lower limit of the inner diameter and outer diameter of the disk is set to 1 mm, and the lower limit value of some outer diameters is larger because the structure requires. The minimum thickness of the disc is set at 5 mm, because too thin a disc is not conducive to the design of subsequent rotor testers. The upper limit of disk parameters is also preliminarily selected according to the shape of the prototype rotor, and should not be too large. The overall guaranteed mass and moment of inertia distribution is similar to that of the prototype engine.

To reduce manufacturing complexity, the hollow tie-rod shaft was redesigned as a solid configuration, increasing total rotor mass by 12.5%. Theoretical analysis confirmed that this modification would elevate the first critical speed by 9.2% if uncompensated (from 7913 rpm to 8645 rpm). However, through multi-variable co-optimization targeting mass redistribution (e.g., −15% axial compressor hub inner diameters) and stiffness balancing (e.g., +8% turbine disk thickness).

4. Optimization Iteration

4.1. Optimization Strategy

An GA optimization program was developed using MATLAB. At the initial stage of program execution, the population is randomly initialized, and MATLAB automatically triggers a background process to call the program. Subsequently, ANSYS is utilized to compute the first three critical speeds of all individuals in the population. Through batch processing scripts, ANSYS writes key parameters such as forward/backward whirling frequencies and resonant frequencies for each order into a designated text file upon termination of each iterative calculation.

MATLAB then extracts these characteristic parameters from the file and calculates the fitness value of each individual based on the optimization objective function. Individuals are ranked according to their fitness values. Finally, selection, crossover, mutation, and reinsertion operations are performed based on fitness to generate a new population. The algorithm automatically terminates and outputs the globally optimal parameter combination when the number of iterations reaches the predefined maximum limit. The complete logical framework of this optimization process is illustrated in **Figure 5**.

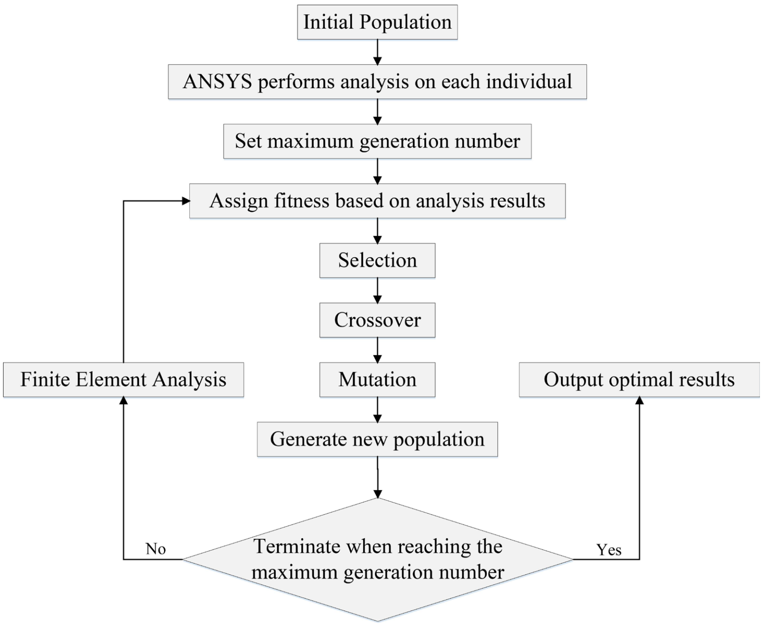

Figure 5. Flowchart of the optimization iteration process.

4.2. Optimization Process

For the optimization design objectives, the GA-based optimization program was configured with 15 design variables, a population size of 20, and a maximum iteration limit of 200 generations. To address the challenge of high-dimensional optimization design variables and enhance convergence efficiency while avoiding local optima traps, the generation gap was set to 0.8 and the mutation rate to 0.07.

The population size (N = 20) was determined through preliminary sensitivity analysis to balance computational efficiency and solution diversity, while the mutation rate (0.07) was selected based on Goldberg's recommendation for medium-dimensional problems [9].

The initial geometry of the prototype rotor before optimization is displayed in **Figure 6**, and the iterative optimization process is illustrated in **Figure 7**. After each optimization iteration, the allowable ranges of optimization variables were

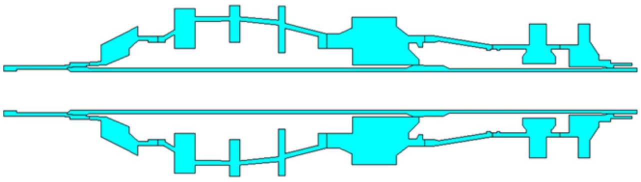

Figure 6. Prototype rotor geometry.

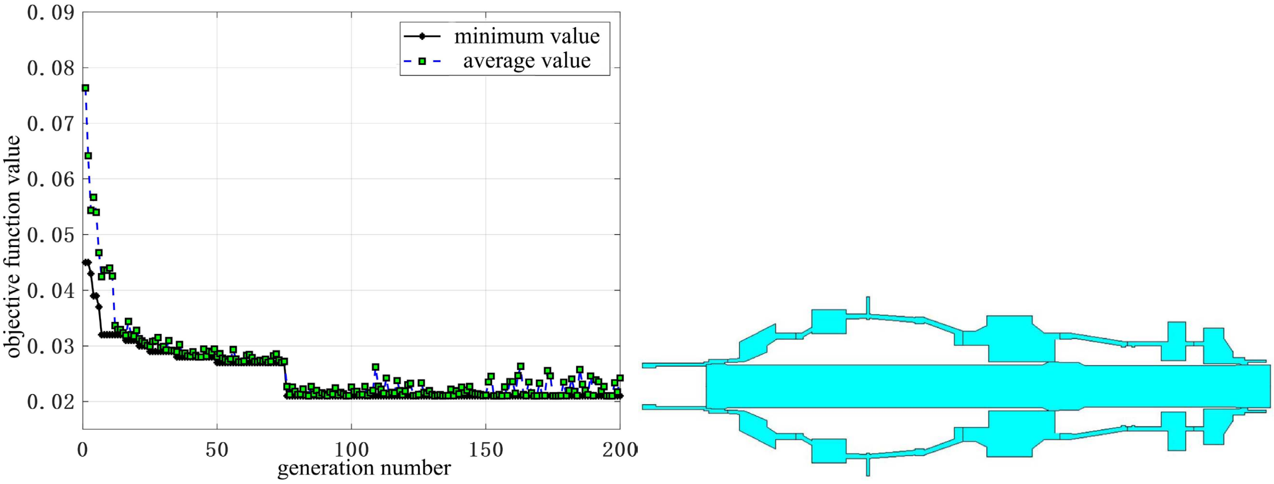

(a) 1st Optimization Cycle

(b) Post-Optimulation Geometry (1st Iteration)

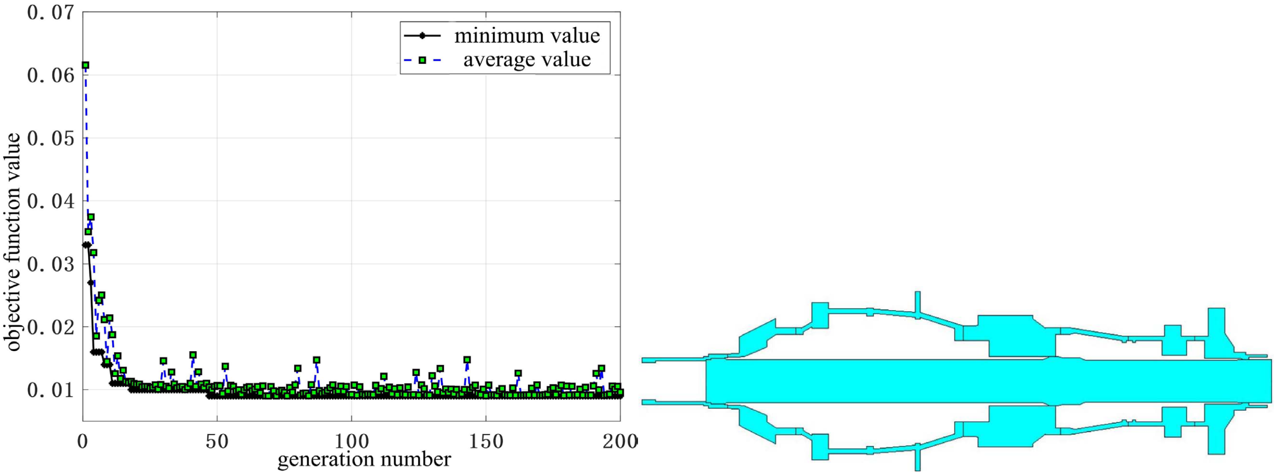

(c) 2nd Optimization Cycle

(d) Post-Optimulation Geometry (2nd Iteration)

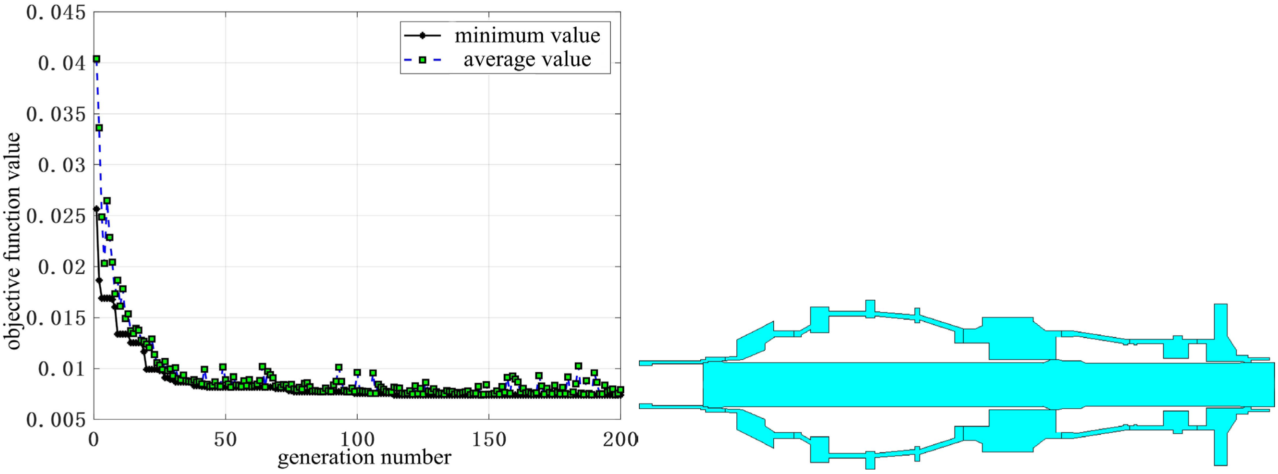

(e) 3rd Optimization Cycle

(f) Post-Optimulation Geometry (3rd Iteration)

Figure 7. Optimization workflow and post-optimization rotor geometry.

dynamically adjusted through an adaptive mechanism: if a parameter value exceeded 95% of its current range for two consecutive iterations, the corresponding bound was expanded by 10% to avoid search space confinement. For example, the outer diameter of the centrifugal compressor disc (H4) initially ranged from 12 - 30 mm. During iteration 1, W4 reached 29 mm (94.4% of its upper limit), prompting an expansion to 31.8 mm. This strategy ensured continuous exploration while adhering to manufacturing constraints.

The objective function value of the model rotor was reduced from 0.021 (initial optimization) to 0.007 (final iteration) through the GA-driven process. During optimization, the axial compressor exhibited a rearward mass shift alongside inner diameter reduction at disk hubs to clearance limits, while the centrifugal compressor retained stable mass distribution. Concurrently, the turbine experienced mass redistribution toward the rear section.

As shown in Table 2, the optimized rotor achieves first three critical speeds of 7838 rpm, 15,487 rpm, and 55,877 rpm, with relative deviations of 0.95%, 0.98%, and 0.28% from the prototype, respectively. Abaqus Explicit dynamics simulations under identical boundary conditions yielded critical speeds of 7852 rpm, 15,410 rpm, and 55,790 rpm, deviating by ≤0.5% from ANSYS results, confirming solver independence.

Table 2. Range of values for design variables.

order	Optimized Rotor, rpm	Prototype Rotor, rpm	Error
1	7838	7913	0.95%
2	15,487	15,337	0.98%
3	55,877	55,721	0.28%

Figure 8 demonstrates identical critical mode shapes between the optimized rotor and the prototype:

1st & 2nd modes: Predominantly exhibit pitching mode characteristics.

3rd mode: Dominated by bending deformation, aligned with the prototype's dynamic behavior.

(a) Prototype Rotor-1st Mode Shape (b) Optimized Rotor-1st Mode Shape

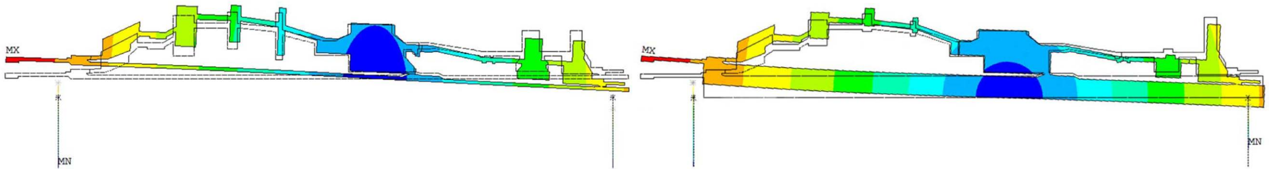

(c) Prototype Rotor-2nd Mode Shape (d) Optimized Rotor-2nd Mode Shape

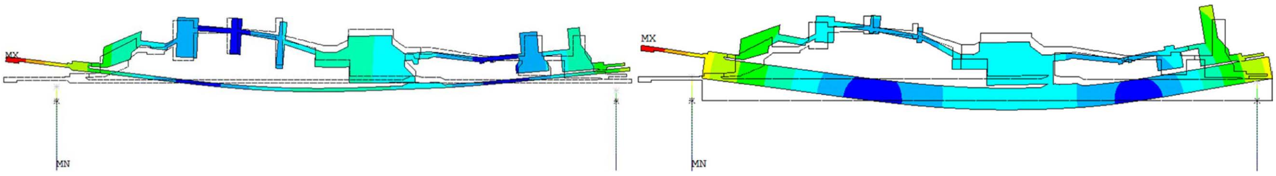

(e) Prototype Rotor-3rd Mode Shape

(f) Optimized Rotor-3rd Mode Shape

Figure 8. Mode shape comparison: prototype vs. optimized rotor.

5. Conclusions

This study proposed a genetic algorithm-enhanced dynamic similarity design framework for multi-stage aero-engine rotors, achieving three pivotal outcomes:

1) Critical speed prediction accuracy was improved to sub-1% errors (0.95%, 0.98%, 0.28%), fulfilling aviation industry requirements.

2) Full modal consistency (MAC > 0.98) between the optimized and prototype rotors was demonstrated, even after structural redesign.

3) The cross-platform co-simulation reduced computational costs, enabling rapid design iterations.

These advancements address the longstanding challenge of dynamic mismatch in multi-stage rotor systems. Future research should prioritize:

Nonlinear Support Modeling: Integrating squeeze-film damper dynamics to capture nonlinear vibration phenomena.

Multi-Physics Coupling: Developing thermo-mechanical similarity criteria for high-temperature rotor applications.

By bridging the gap between simplified models and real-world complexity, this work lays a foundation for next-generation adaptive rotor design.

Conflicts of Interest

The authors declare no conflicts of interest regarding the publication of this paper.

References

[1] Ding, S., He, Y. and Zheng, X. (2021) A Probabilistic Approach for Three-Dimensional Variation Analysis in Aero-Engine Rotors Assembly. *International Journal of Aeronautical and Space Sciences*, **22**, 1092-1105. https://doi.org/10.1007/s42405-021-00384-w

[2] Chen, G. (2015) Vibration Modelling and Verifications for Whole Aero-Engine. *Journal of Sound and Vibration*, **349**, 163-176. https://doi.org/10.1016/j.jsv.2015.03.029

[3] Sykes, J.E.H. and Holrnes, R. (1990) The Effects of Bearing Misalignment on the Nonlinear Vibration of Aero-Engine Rotor-Damper Assemblies. *Proceedings of the Institution of Mechanical Engineers*, *Part G*: *Journal of Aerospace Engineering*, **204**, 83-99. https://doi.org/10.1243/PIME_PROC_1990_204_215_02

[4] Sever, I.A. (2016) Nonlinear Vibration Phenomena in Aero-Engine Measurements. In: *Dynamics of Coupled Structures*, *Volume* 4: *Proceedings of the* 34*th IMAC*, *A Conference and Exposition on Structural Dynamics* 2016, Springer International Publishing, 241-252. https://doi.org/10.1007/978-3-319-29763-7_23

[5] Liu, Y.F., Wang, Q.W., Wang, S.Y., Zhang, S., Cao, J.M. and Zhou, C.J. (2014) The Analysis and Diagnosis of Vibration Fault of a Certain Type of Aero-Engine. *Applied Mechanics and Materials*, **633**, 1256-1262. https://doi.org/10.4028/www.scientific.net/AMM.633-634.1256

[6] Holmes, R. and Sykes, J.E.H. (1996) The Vibration of an Aero-Engine Rotor Incorporating Two Squeeze-Film Dampers. *Proceedings of the Institution of Mechanical Engineers, Part G: Journal of Aerospace Engineering*, **210**, 39-51. https://doi.org/10.1243/PIME_PROC_1996_210_343_02

[7] Luo, Z., Li, L., He, F. and Yan, X. (2021) Partial Similitude for Dynamic Characteristics of Rotor Systems Considering Gravitational Acceleration. *Mechanism and Machine Theory*, **156**, Article 104142. https://doi.org/10.1016/j.mechmachtheory.2020.104142

[8] Wang, A.L. and Huang, L.K. (2012) Research on Similarities between Abnormal Rotor Model and the Prototype Based on Dynamic Similarity. *Advanced Materials Research*, **591**, 1991-1995. https://doi.org/10.4028/www.scientific.net/AMR.591-593.1991

[9] Goldberg, D.E. and Richardson, J. (1987) Genetic Algorithms with Sharing for Multimodal Function Optimization. In: *Genetic Algorithms and Their Applications: Proceedings of the Second International Conference on Genetic Algorithms*, Vol. 4149, 414-425.